

Particulate matter (PM₁₀) in Istanbul: Origin, source areas and potential impact on surrounding regions

M. Koçak^a, C. Theodosi^a, P. Zarmas^a, U. Im^a, A. Bougiatioti^a, O. Yenigun^b, N. Mihalopoulos^{a,*}

^a Environmental Chemical Processes Laboratory, Department of Chemistry, University of Crete, P.O. Box 2208, 71003 Heraklion, Greece

^b Bogaziçi University, Institute of Environmental Sciences, Hisar Campus, 34342 Bebek, Istanbul, Turkey

ARTICLE INFO

Article history:

Received 17 May 2010

Received in revised form

26 August 2010

Accepted 5 October 2010

Keywords:

Istanbul

Source apportionment

Potential source contribution function

PM₁₀

ABSTRACT

Water-soluble ions (Cl⁻, NO₃⁻, SO₄²⁻, C₂O₄²⁻, Na⁺, NH₄⁺, K⁺, Mg²⁺, Ca²⁺), water soluble organic carbon (WSOC), organic and elemental carbon (OC, EC) and trace metals (Al, Ca, Ti, V, Cr, Mn, Fe, Ni, Cu, Zn, Cd and Pb) were measured in aerosol PM₁₀ samples above the megacity of Istanbul between November 2007 and June 2009. Source apportionment analysis using Positive Matrix Factorization (PMF) indicates that approximately 80% of the PM₁₀ is anthropogenic in origin (secondary, refuse incineration, fuel oil and solid fuel combustion and traffic). Crustal and sea salt account for 10.2 and 7.5% of the observed mass, respectively. In general, anthropogenic (except secondary) aerosol shows higher concentrations and contributions in winter. Mean concentration and contribution of crustal source is found to be more important during the transitional period due to mineral dust transport from North Africa. During the sampling period, 42 events exceeding the limit value of 50 µg m⁻³ are identified. A significant percentage (91%; n = 38) of these exceedances is attributed to anthropogenic sources. Potential Source Contribution Function analysis highlights that Istanbul is affected from distant sources from Balkans and Western Europe during winter and from Eastern Europe during summer. On the other hand, Istanbul sources influence western Black Sea and Eastern Europe during winter and Aegean and Levantine Sea during summer.

© 2010 Elsevier Ltd. All rights reserved.

1. Introduction

During the last two decades, urban air pollution has been recognized as one of the world's major environmental issues, particularly in megacities (Yusuf and Resosudarmo, 2009 and references therein). Recently, air pollution from megacities has attracted substantial scientific interest owing to their potential impact on regional and global climate (Lawrence et al., 2007; Duh et al., 2008; Favez et al., 2008).

Being one of the largest cities in Europe, Istanbul has demonstrated an extravagant urban growth since 1970s (Tayanc et al., 2009). Urbanization continuously increased and Istanbul grew from a city of 2 million in 1970 to a megacity of 12.5 million in 2007 (TUIK, 2007). Air pollution has emerged as one of the most important environmental problems in Istanbul owing to growth in population, use of poor quality fuel, poor quality burning devices, application of ineffective burning technologies in industry and insufficient efforts on reducing traffic emissions (Istanbul Air

Quality Strategy, 2009). Local emissions, especially from road traffic are found to be a major source of particulate matter (Markakis et al., 2009) and maximize in winter (Im et al., 2010). Additionally, contribution of air pollutants via long range transport (mainly from Eastern Europe) could be as important as local sources (Kindap et al., 2006; Karaca and Camci, 2010).

One of the main concerns in megacities is atmospheric aerosol (or particulate matter, PM) since it affects air quality and public health. PM₁₀ is defined as particles with a diameter smaller than 10 µm. Considering their potential adverse health and environmental impacts, legislation of the PM concentration limits has been established worldwide. In the European Union, the annual and daily PM₁₀ limits have been set to 40 µg m⁻³ and 50 µg m⁻³ (which could only be exceeded for 35 days), respectively, while annual PM_{2.5} (particles with a diameter smaller than 2.5 µm) value has been limited to 17 µg m⁻³ (Directive, 2008/50/EC of the European Parliament and the Council of 21 May 2008 on ambient air quality and cleaner Europe). To determine the origin of aerosols in Istanbul, a source apportionment study has been performed by applying positive matrix factorization (PMF). Exceedances in PM₁₀ values have been investigated with respect to origin and chemical composition. In addition, potential regions affecting Istanbul and

* Corresponding author. Fax: +30 2810 393601.

E-mail address: mihalo@chemistry.uoc.gr (N. Mihalopoulos).

being affected by Istanbul have been identified by using the potential source contribution function.

2. Materials and methods

2.1. Aerosol sampling and measurements

Daily aerosol filters were obtained from a site located on the roof of the Institute of Environmental Sciences of Boğaziçi University (41.09 N, 29.05 E, 80 m above sea level, see Fig. 1), on the western side of the Bosphorus, Istanbul from November 2007 to June 2009. The Sea of Marmara, the Black Sea and the Bosphorus channel controls the general climate of the greater Istanbul region. Usually, Istanbul has a Mediterranean type of climate and hence it is warm and dry in summer and cold and wet in winter. This is mainly because of the difference in air mass flow coming from the Balkan Peninsula and the Black Sea (Incecik, 1996). The sampling site is relatively far from industrial activities, but only a few hundred meters away from the Bosphorus strait where heavy international shipping and local passenger ferries are active throughout the year. Furthermore, the Fatih Sultan Mehmet Bridge, which connects the two sides of the city, lies only a few hundred meters away from the Institute. Motorway traffic and the transit ships passing through the Bosphorus strait are the main anthropogenic aerosol sources in the vicinity of the sampling site (Theodosi et al., 2010b). The representativeness of the sampling site for the Greater Istanbul Area has been tested by Theodosi et al. (2010b). The measured PM₁₀ levels were compared with those obtained by the Istanbul Greater Municipality Air Quality Network (IGMAQN) at 9 urban and street-canyon stations across Istanbul (Aksaray, Alibeykoy, Besiktas, Esenler, Kartal, Sariyer, Umraniye, Uskudar and Yenibosna). This study showed that measurements at Boğaziçi University generally captured not only the seasonal (slope = 0.97, R² = 0.77) but also the day-to-day variability (Theodosi et al., 2010b).

A total of 212 polycarbonate and 113 Quartz filters were collected. The sampling was carried out unequally therefore, different number of samples was collected from each month and season. Samples obtained in winter and summer covered 35% and 45% of the samples whereas; only 20% of the samples were collected in summer. Using polycarbonate filters, PM₁₀ concentrations were determined gravimetrically, water-soluble ions (Cl⁻, NO₃⁻, SO₄²⁻, C₂O₄, Na⁺, NH₄⁺, K⁺, Mg²⁺ and Ca²⁺) were measured by

ion chromatography, WSOC (water-soluble organic carbon) was determined by an organic analyzer (TOC-V_{CSH}, Shimadzu), and trace metals (Al, Ca, Ti, V, Cr, Mn, Fe, Ni, Cu, Zn, Cd and Pb) were analyzed by Inductively Coupled Plasma–Mass Spectrometry X-series. Quartz filters were used to analyze OC and EC with the Thermal–Optical Transmission (TOT) technique (Birch and Cary, 1996), using a Sunset Laboratory OC/EC Analyzer (for more details on sampling and measurements see Bardouki et al., 2003; Koulouri et al., 2008 and Theodosi et al., 2010a). WIOC (water insoluble organic carbon) values were calculated by subtracting the WSOC from TOC WIOC = OC – WSOC). Except Cr and V (~8%), blank contributions were found to be less than 5% for all measured species. Uncertainties for trace metal and remain species were better than 15% and 10%, respectively.

2.2. Air mass back/forward trajectories

Backward and forward trajectories from and to the Istanbul sampling site were computed by the HYSPLIT Dispersion Model (Hybrid Single Particle Lagrangian Integrated Trajectory; Draxler and Hess, 1998) and illustrated by 1-h endpoint locations in terms of latitude and longitude. The choice of arrival (or starting) height was based on the boundary layer heights obtained from the Weather Research and Forecast (WRF 3.1.) mesoscale meteorological model (not presented here) that has been driven employing National Centers for Environmental Prediction (NCEP) reanalyses data on 1° resolution. As expected, boundary layer showed variability from one month to another. Boundary layer in winter (for example, December and January) was found to be as high as 1300 m and it ranged mostly between 700 and 800 m whereas, boundary layer in transition (for instance, March and April) reached up to 2500 m with values ranging mainly from 800 to 1400 m. Hence, 3-day backward and forward trajectories of air masses at a height of 1000 m were calculated between November 2007 and June 2009.

2.3. Source apportionment by positive matrix factorization

Positive matrix factorization (PMF2 version 4.2, hereinafter referred to as 'PMF') was utilized to characterize sources of PM₁₀ concentration in Istanbul. PMF was developed by Paatero and Tapper (1994) and described in detail by Paatero (2007). PMF is a powerful receptor modeling tool, which has been shown to successfully assess each source contribution to particulate matter (Paatero and Tapper, 1994; Huang et al., 1999; Lee et al., 1999; Viana et al., 2008; Koçak et al., 2009). PMF constrains factor loadings and factor scores to non-negative values. Another advantage of the PMF is its ability to handle missing data and values below detection limits by adjusting the corresponding error estimates. In PMF any data matrix X having n rows (number of samples) and m columns (number of species) can be factorized into two matrices, namely G (n × p) and F (p × m) and the residual part E, where p denotes the number of factors extracted.

$$X = GF + E \quad (1)$$

G is the source contribution matrix with extracted sources (factors) and F is a source profile matrix.

Uncertainties of measured data were assessed as the sum of the analytical uncertainties and 1/3 of the detection limit value. Values below the detection limit and missing data were replaced by half of their detection limit and by their mean values, respectively. Uncertainties for values below the detection limit were set at 5/6 of the detection limit whilst uncertainties of the missing data (particularly OC and EC) were adjusted to four times their mean concentrations (Polissar et al., 1998). In the concurrent analysis

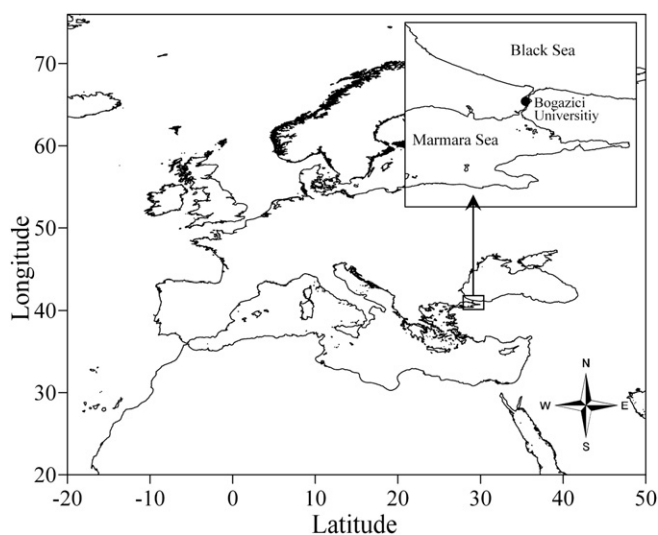


Fig. 1. Location of sampling site, Bogazici University, Istanbul.

a 196×24 matrix (196 days and 24 species) was used to identify aerosol sources. The robust mode of PMF has been applied for analyzing the dataset. It can avoid excessively large values in the dataset, which can disproportionately affect the results. The parameter α is referred to as the outlier distance. Data values lying more than α standard deviations above or below the fitted value will be treated as outliers and receive a decreased weight in PMF. Values of 2.0, 4.0 and 8.0 were suggested by Paatero (2007) for outlier distance to achieve easier comparison of results obtained by different researchers. During the application of PMF the value $\alpha = 4.0$, error model-14 and $C_3 = 0.1$ were applied (Lee et al., 1999; Paatero, 2007). The PMF program allows repetition of the analysis from random starting points to test if a global minimum solution is achieved. For this purpose, the analysis was allowed to repeat ten times from ten pseudo-random starting points and the Q values were not very different from each other. PMF was run with different Fpeak values to explore the rotational freedom after identifying the number of factors. A rotational matrix (Rotmat) in PMF is utilized to reveal if factors have rotational freedom (Lee et al., 1999). Taking into account the variation in the Q value and the largest element in Rotmat, the Fpeak value was adjusted to 0.2.

Although, there is no mathematical criterion to identify the correct number of species, theoretical Q [$Q_{\text{expected}} = nm - p(n + m)$] and scaled species residuals can be helpful. Seven factors were identified by PMF with a Q value of 4507 ($Q_{\text{expected}} = 3164$ for seven factors) and scaled residuals were found to be randomly distributed between -2 and 2 . The decrease in the number of factors resulted in a combination of distinct sources (and higher Q value). For example, six factors were not able to characterize the secondary (Factor-1) aerosol group with a maximum in summer. On the contrary, the increase in the number of factors caused the dissociation of secondary aerosol (particularly sulfate and ammonium) (Factor-1) into two different sources.

2.4. Potential source contribution function (PSCF) and potential impact (PI)

A 2° longitude \times 2° latitude grid has been superimposed over the region defined by 20° N- 76° N and 20° W- 50° E. The residence time and special residence time analysis then were calculated using the formula given by Ashbaugh et al. (1985):

$$P[A_{ij}] = \frac{n_{ij}}{N} \tag{2}$$

$$P[B_{ij}] = \frac{m_{ij}}{N} \tag{3}$$

where n_{ij} is the number of trajectory segment endpoints that fall in the ij^{th} cell during a time interval T, m_{ij} is the number of segment points in the ij^{th} cell for those trajectories, which arrive at the receptor site (back trajectories) when the aerosol species concentration is higher than the threshold values, N is the total number of endpoints computed for the time interval, $P[A_{ij}]$ and $P[B_{ij}]$ represent the residence time probability of the randomly selected air parcel in the ij^{th} cell relative to the total time interval T and special residence time probability, respectively. Subsequently potential source contribution functions (PSCF) were evaluated by dividing $P[B_{ij}]$ with $P[A_{ij}]$.

A similar approach was adopted to determine potential impact (PI) of Istanbul on surrounding regions applying forward trajectories and Eqs. (2) and (3), where n_{ij} is the number of trajectory segment endpoints that fall in the ij^{th} cell during a time interval T, m_{ij} is the number of segment points in the ij^{th} cell for those

trajectories which leave from the receptor site (forward trajectories) when the aerosol species concentration is higher than the threshold values and N being the total number of endpoints computed.

The study domain covers area between 20° N- 76° N and 20° W- 50° E therefore it consists of 980 cells $2 \times 2^\circ$ in latitude and longitude. The total number of trajectory endpoints located in the grid is found to be 11 878 with an average value of 12 endpoints per cell. For each defined sources, approximately 40 daily trajectories out of 196 arriving at (or leaving from) Istanbul were used to evaluate PSCF (or PI) which accounted for around 20% of the total trajectories. It is likely that a small number of end points in a grid cell may result in high potential probabilities. In order to reduce the effect of small values of n_{ij} , the PSCF and PI values were down weighted using an arbitrary weighting function. An arbitrary weighting function was applied when the number of the end points in a particular cell was less than three times the average number of end points for all cells (Polissar et al., 2001; Kim and Hopke, 2006). Thus, the weighting functions were assigned as follows:

$$W_{ij} = \begin{cases} 1.0 & 36 < n_{ij} \\ 0.8 & 27 < n_{ij} \leq 36 \\ 0.6 & 18 < n_{ij} \leq 27 \\ 0.4 & 9 < n_{ij} \leq 18 \\ 0.2 & n_{ij} \leq 9 \end{cases} \tag{4}$$

3. Results and discussion

3.1. PMF2 source apportionment for PM₁₀

Seven factors have been identified using PMF2 for PM₁₀ samples collected at Istanbul. A comparison between daily reconstructed PM₁₀ mass contributions from all factors versus measured PM₁₀ values showed that extracted factors successfully mimic the measured PM₁₀ levels (slope = 1.01; intercept = 0.72 and $R^2 = 0.98$; Fig. 2). The intercept is found to be 0.72 and the unknown fraction accounts only for 2% of the PM₁₀. The defined seven factors explain 98% of the PM₁₀ mass and are depicted in Fig. 3.

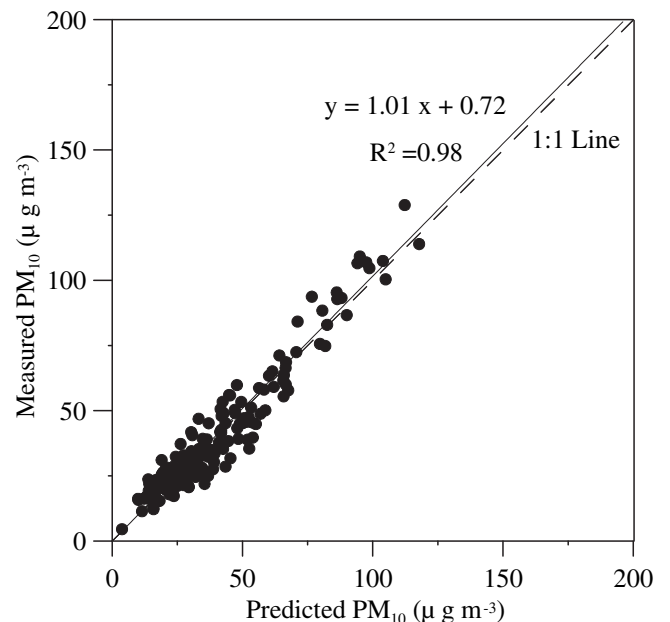


Fig. 2. Comparison of observed daily levels and predicted form PMF for PM₁₀.

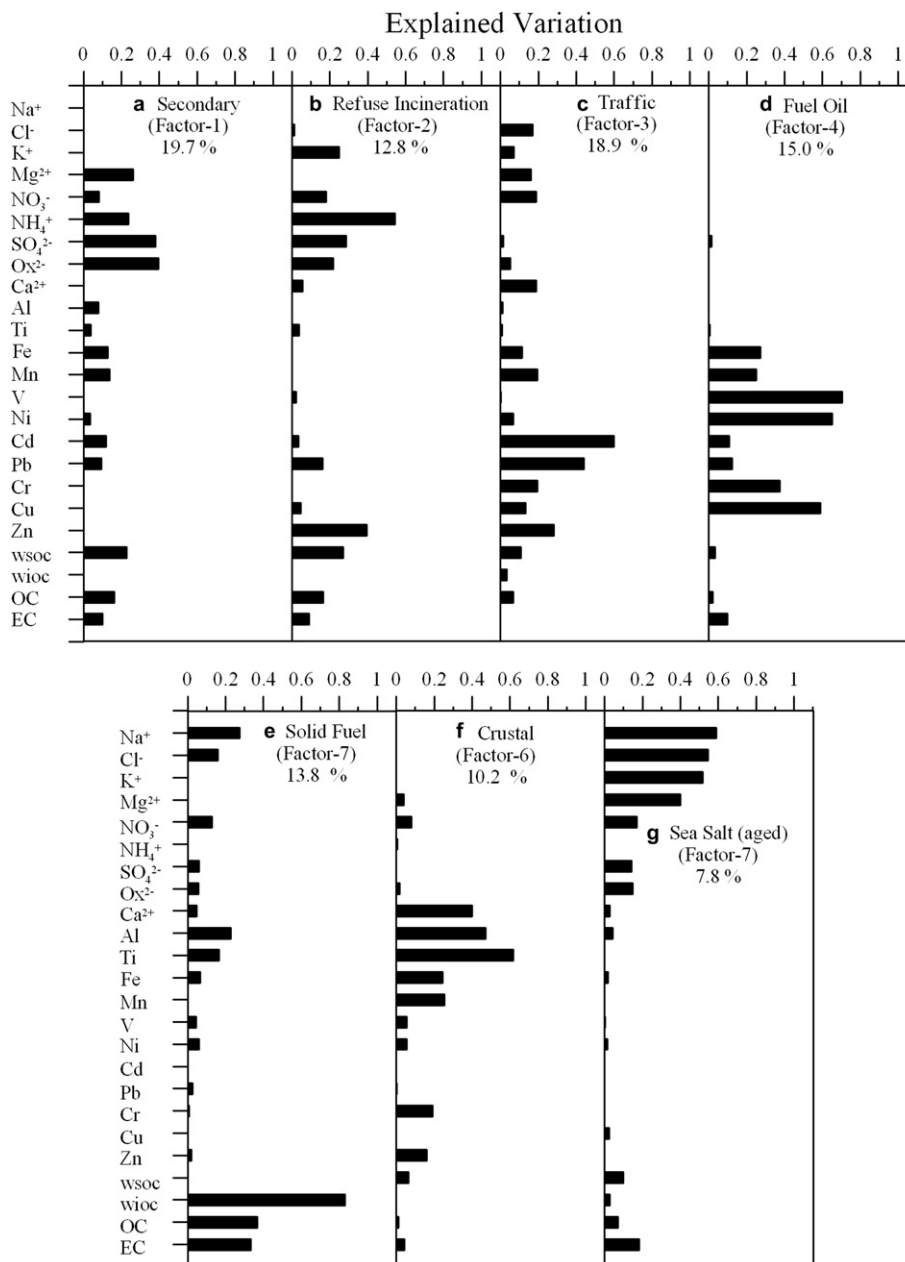


Fig. 3. Source profiles for PM₁₀ from PMF.

The first two factors (Fig. 3a, b) are mainly characterized by NH_4^+ , SO_4^{2-} , C_2O_4 and WSOC. However, these two factors show distinct difference in their source profiles. First, the calculated equivalent ratios of NH_4^+ and SO_4^{2-} are found to be 0.42 and 1.02 for factors 1 and 2, respectively. These ratios imply that sulfate is not sufficiently neutralized by ammonium in the first factor while completely neutralized [$(\text{NH}_4)_2\text{SO}_4$] in the second factor. In addition, the second factor is associated with K^+ ($\text{EV} \sim 0.25$) and Zn ($\text{EV} \sim 0.4$), which can be attributed to refuse incineration (Morishita et al., 2006; Lim et al., 2010). On the other hand, an examination of the factor contribution plots (see Fig. 4b, c) reveals a summer maximum for the first factor contrasting the winter maximum of the second one. Therefore, considering the summer peak and the source profile, the first factor could be attributed to secondary aerosol formation due to increased photochemical activity. The second factor might be characterized as refuse incineration (e.g. municipal) since it shows winter maxima

and have loadings of K^+ and Zn . First and second factors explain 19.7 and 12.8% of the PM₁₀ mass, respectively.

The third factor (Fig. 3c) is primarily composed by Cd , Pb and mixed with Cl^- , K^+ , NO_3^- and trace elements (such as Zn , Cu , Cr , Mn , Fe and Ca). Previous studies have shown emissions of Cl^- and NO_3^- originating from motor vehicles (Raman and Hopke, 2007; Lim et al., 2010) and Zn from tires/brakes and lubricating oil mixed with gasoline for two-stroke engines of motorcycles (Begum et al., 2004; Hien et al., 2005). This source also has contributions from Ca , Fe and Mn which are mostly attributed to road dust (Lee et al., 1999; Morishita et al., 2006). Thus it might be attributed to traffic and accounts for 18.9% of the measured PM₁₀.

The fourth factor (Fig. 3d) is mainly characterized by Ni , V , Cu and mixed with Fe , Mn , Cd , Pb , Cr . Based on these elements the assigned source is fuel oil and represents 15.0% of the PM₁₀ concentration (Koçak et al., 2009).

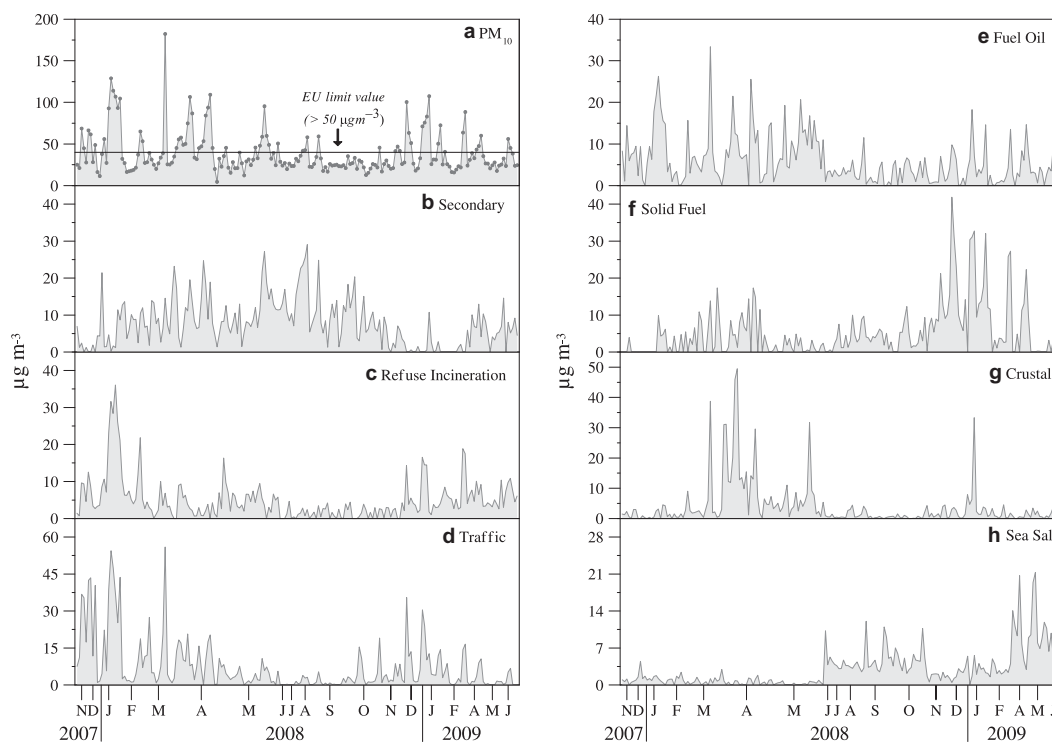


Fig. 4. Daily variability of the PM₁₀ and each source.

The fifth factor (Fig. 3e) predominantly consists of WIOC, OC, EC and mixed with a small amount of trace elements, nitrate, sodium and chlorine. Favez et al. (2008) have shown that WIOC originates mainly from fossil fuel primary source in winter. Consequently, this factor could be attributed to primary emissions from burning processes (solid fuel burning; e.g. wood). Its contribution to PM₁₀ is found to be 13.8%.

The sixth factor (Fig. 3f) principally consists of Ti, Al, Ca, Fe, Mn, and Cr. For this factor, Fe/Al ($=6.2 \times 10^{-1}$) and Ti/Al ($=5.3 \times 10^{-2}$) ratios are found to be higher than those for upper crust (Wedepohl, 1995; Fe/Al = 4.0×10^{-1} and 4.0×10^{-2}) whereas close to Saharan end member (Andreae et al., 2002; Fe/Al = 6.3×10^{-1} and 5.7×10^{-2}). Therefore this factor could be characterized as crustal material and elucidates 10.2% of the PM₁₀.

The seventh factor (Fig. 3g) mainly consists of Na⁺, Cl⁻ and K⁺. It might be attributed to aged sea salt as it has a lower Cl/Na ratio than that observed in pure seawater and associated with nss-SO₄²⁻, NO₃⁻, C₂O₄ and WSOC. This source explains 7.8% of the observed PM₁₀.

3.2. Temporal variability of PM₁₀ and aerosol sources

For the period between November 2007 and June 2009 the daily variations of the concentrations and seasonal mean values for PM₁₀ as well as aerosol sources contributions are depicted in Fig. 4 and Table 1, respectively. The PM₁₀ concentrations and aerosol sources showed substantial daily variability in agreement with previous studies carried out in the Mediterranean region (Rodriguez et al., 2002; Gerasopoulos et al., 2006; Koçak et al., 2007a, b). The seasonality of PM₁₀ and the determined aerosol sources in Istanbul are tested statistically by applying the Wilcoxon test at the 95% confidence interval. As stated before (see Section 2.1), usually Istanbul has a Mediterranean type climate. Its climate is characterized by mild, humid winters and dry summer. Winter months are dominated by rainfall whereas the months are characterized by the lack

of wet precipitation. The transition seasons, spring and autumn are of very different lengths. The relatively long spring season (March–May) is characterized by unsettled winter type weather, associated with North African cyclones. Autumn usually lasts one month (October) and is characterized by an abrupt change from the summer to the unsettled weather of winter (Brody and Nestor, 1980). Hence, considering features described above, the annual period are defined by three seasons: Winter (January, February, November and December), Transitional (March, April, May and October) and Summer (June, July, August and September). The following general observations may be made:

- PM₁₀ levels exhibit no statistical significant difference between winter (mean = $44.5 \mu\text{g m}^{-3}$) and transitional period (mean = $41.76 \mu\text{g m}^{-3}$) whilst they are found to be lowest in summer (mean = $28.6 \mu\text{g m}^{-3}$; see Fig. 4a and Table 1). Enhanced concentrations of PM₁₀ during winter and summer are associated predominantly with intense pollution and to a lesser extent with mixed and/or sporadic peaks of mineral dust events (for more details see Section 3.3).
- Traffic, solid fuel and refuse incineration sources were found to be higher in winter than the other seasons, accounting for 28.5, 18.8 and 17.8% of PM₁₀ mass, respectively, in winter. High

Table 1
Seasonal variations in PM₁₀ and aerosol sources ($\mu\text{g m}^{-3}$) observed in Istanbul.

Species	Winter	Transition	Summer
PM ₁₀	44.5	39.1	29.8
Contributions from each source (%)			
Secondary	3.2 (7.2%)	9.5 (24.3%)	11.4 (38.1%)
Refuse Incineration	7.9 (17.8%)	3.9 (10.0%)	2.6 (8.7%)
Traffic	12.7 (28.5%)	6.3 (16.1%)	1.2 (3.9%)
Fuel Oil	5.4 (12.2%)	7.3 (18.7%)	3.4 (11.4%)
Solid Fuel	8.4 (18.8%)	3.9 (10.1%)	3.7 (12.6%)
Crustal	2.2 (4.9%)	6.5 (16.6%)	1.2 (3.9%)
Sea Salt	1.8 (4.1%)	2.9 (7.5%)	4.9 (16.4%)

pressure systems, temperature inversions and low wind speed occurring during winter can explain the appearance of the winter maxima, in agreement with the observations of Inceciç (1996).

- c) The crustal source shows statistically significant decreasing concentration in the order of Transition > Winter > Summer. The highest contribution to PM₁₀ is found to be ~17% during spring when air mass trajectories originated mainly from North Africa with sporadic peaks of mineral dust (Alpert and Ziv, 1989; Kubilay and Saydam, 1995; Moulin et al., 1998; Kubilay et al., 2000, 2005; Koçak et al., 2004a).
- d) As expected, the mean concentrations of secondary aerosol source are found to be larger in summer and transitional than in winter, the difference being statistically significant (at 95% confidence interval). Although, there is no statistical difference between summer and transitional period, secondary aerosol contribution gradually increases from winter to summer due to enhanced photochemistry which favors gas to particle conversion processes in the area (Mihalopoulos et al., 2007; Koçak et al., 2004b). Its contribution to PM₁₀ is found to be 1.6 and 5.3 times higher in summer (38.1%) than during transition (24.3%) and winter (7.2%) periods, respectively. Similarly, sea salt source demonstrates highest mean concentration in summer (statistically significant at 95% confidence interval) and may be attributed to prevailing north-western winds from Black Sea (Theodosi et al., 2010b). Sea salt contribution in summer (16.4%) is two to four times higher than during transitional (7.5%) and winter (4.1%) periods, respectively.

3.3. PM₁₀ exceedances at Istanbul

A number of studies have focused on the origin of the exceedances in PM₁₀ in the Mediterranean (Artinano et al., 2001; Rodriguez et al., 2002; Koçak et al., 2007a). These studies have indicated that exceedances of PM₁₀ might also originate from natural sources such as African dust and sea salt. However, natural events have less impact on PM₁₀ exceedances at urban and industrialized sites compared to rural sites.

Fig. 4 depicts time series plots of the measured PM₁₀ and the estimated daily contributions for each of the identified sources. Obtained sources from PMF analysis (see Section 3.1) are used to identify and classify the origin (natural and anthropogenic) of the exceedances. Secondary, refuse incineration, traffic, fuel oil and solid fuel are considered as anthropogenic sources, whereas crustal dust and sea salt as natural sources. During the sampling period 42 events (21% of the samples) are found to exceed the legislative PM₁₀ value established by the EU. From these exceedances, 38 events (91%) were characterized as anthropogenic in origin, 3 events (7%) as mixed and 1 event is attributed to a dust event.

- a) *Anthropogenic* (n = 38): During these events anthropogenic sources contribute from 36 to 124 $\mu\text{g m}^{-3}$ to the PM₁₀ mass concentration, i.e. from 72% to almost 300% of the EU PM₁₀ daily limit value. A characteristic period with an intense anthropogenic influence is from 12th to 17th of January 2008. During this period PM₁₀ values were higher than 90 $\mu\text{g m}^{-3}$ with a maximum value of 129 $\mu\text{g m}^{-3}$ on 13th of January. Source apportionment for January 13th (Fig. 5) shows that anthropogenic sources account for about 90% of the observed PM₁₀, with natural sources contributing only by 3%. Additionally, Im et al. (2010) clearly demonstrated that the episodic period was dominated by anthropogenic sources.
- b) *Mixed events* (n = 3): For three of the observed PM₁₀ exceedances, anthropogenic and natural sources are found to

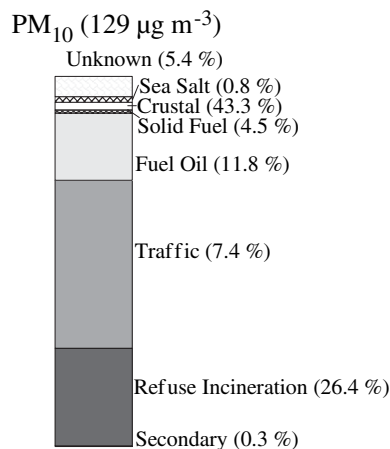


Fig. 5. Source apportionment for PM₁₀ during pollution event on 13th of January 2008.

contribute almost equally. A typical case of mixed event occurred on the 12th of April 2008 with PM₁₀ concentration of (107 $\mu\text{g m}^{-3}$). Source apportionment analysis (Fig. 6) indicated that dust contribution accounts for 43% of PM₁₀ which increases to 44% by adding sea salt. Similarly, anthropogenic sources are found to contribute about 44%. Thus mixing of aerosols from natural and anthropogenic sources is the origin of this PM₁₀ exceedance.

- c) *Dust event* (n = 1): During the whole sampling period only one PM₁₀ exceedance is attributed to a dust event (the 13th of April 2008 with PM₁₀ of 87 $\mu\text{g m}^{-3}$). It is likely that discontinuous sampling strategy results in missing of heavy or strong dust storms due to its episodic nature. Back trajectory analysis at 1000 and 3000 m levels (Fig. 7a) shows that air masses reaching Istanbul originate from the North Africa (particularly from Libyan Desert). The Ozone Mapping Instrument (OMI) image demonstrates a strong mineral dust episode mainly over the Libyan Desert and the Eastern Mediterranean region. The Sahara origin is also verified by the chemical composition of the PM₁₀ (Fig. 7b). The source apportionment shows that 57% of the observed PM₁₀ originates from mineral dust. Pollution sources account for 41% of PM₁₀ whereas sea salt mass contributes only by 1%.

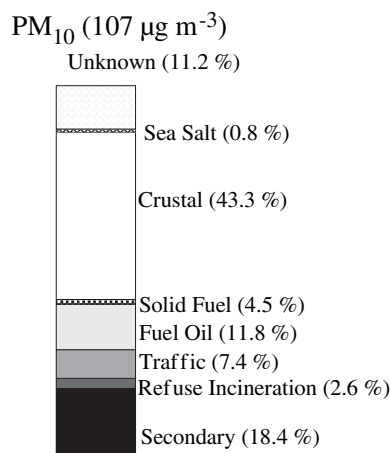


Fig. 6. Source apportionment for PM₁₀ during mixed event on 12th April 2008.

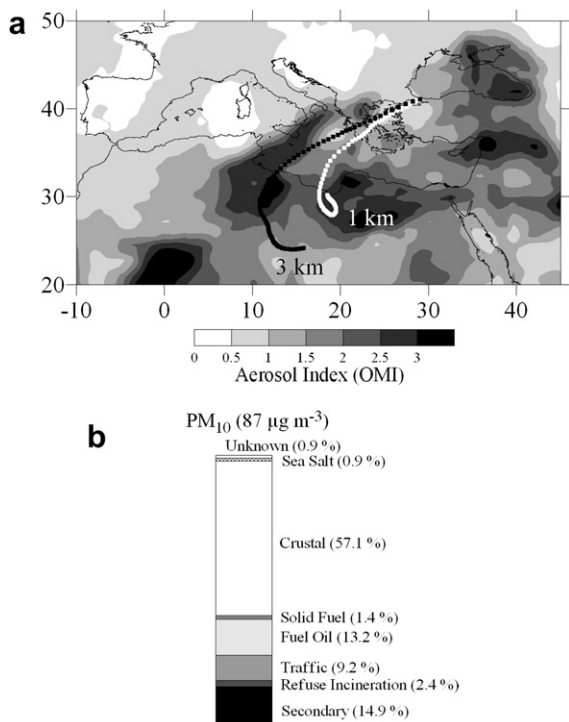


Fig. 7. Saharan dust transport observed on 13th of April 2008: (a) The three-day back trajectories showing the transport of air masses to the sampling site and OMI Absorbing Aerosol Index. (b) Source apportionment for PM₁₀ during Saharan dust events for the 13th of April 2008.

3.4. PSCF and PI analysis for PM₁₀ above Istanbul

Synoptic meteorology, as well as local circulations due to the complex topography of the area, plays an important role in the seasonal transport paths of secondary pollutants (Im et al., 2006, 2008). Black Sea on north and Marmara Sea on south of the city produce a differential heating of surfaces, leading to local circulations that have different diurnal characteristics. In the summer months, the Persian Gulf low pressure system that extends from the southeast of Turkey leads to dominant northeasterly winds that transport air masses from Eastern Europe. Summer months are also influenced by the subtropical Azores high. Typical summer-time trajectories are originated from Balkans and northeastern Europe whereas winter-time trajectories are either originated from Genoa Gulf that moves to the northeast affecting Istanbul and Black Sea, or from western and middle Mediterranean, including Genoa Gulf and north of Sahara Desert that affects Turkey (Karaca et al., 2000).

3.4.1. PSCF for PM₁₀ above Istanbul

To investigate the potential aerosol source regions influencing Istanbul but also the impact of Istanbul to the neighboring regions, potential source function is applied (see Section 2.4). To simplify our analysis, sources showing winter maximum are combined into one group. This group, referred below as Pollution-1, comprises refuse incineration, traffic, fuel oil and solid fuel. In addition, secondary aerosol (Pollution-2) and crustal sources (Crustal) are also considered since the former shows summer maxima and the latter during the transitional period.

a) *Crustal Source*: The PSCF map for crustal source (Fig. 8) showed that the potential sources are located at North Africa in agreement with previous works (Engelstaedter and Washington, 2007; Koçak et al., 2009). From Fig. 8, Libya, Algeria and

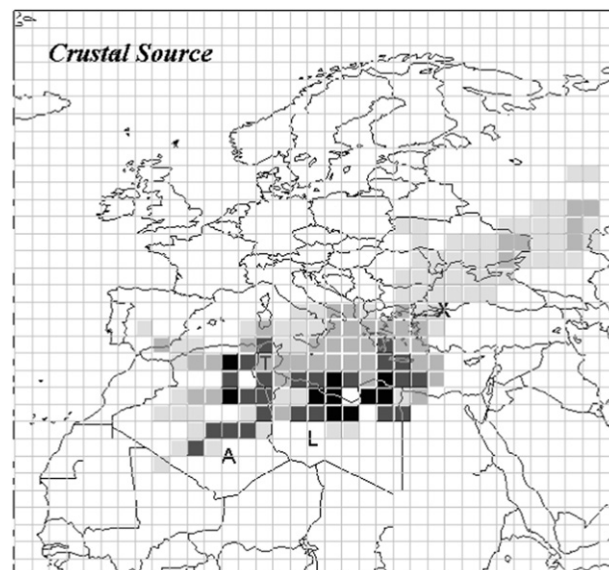


Fig. 8. Distribution of PSCF values for crustal source. X: Sampling site (Istanbul). L: A: Algeria, Libya and T: Tunisia.

Tunisia can be considered as the most important source areas of mineral dust transported to Istanbul.

b) *PSCF for Pollution-1 and Pollution-2*: The PSCF map derived for the Pollution-1 source (see Fig. 9a) denotes that Istanbul is under the influence of several possible source regions. The main source areas are Balkans (including the former Republic of Yugoslavia, Albania, Bosnia, Croatia, Bulgaria and Greece), Austria, Southern Germany, Italy (Central and southeastern) and Central Poland in agreement with the observations of Karaca et al. (2009). These potential sources are also verified by emission data provided by Visschedijk et al. (2007), where the aforementioned countries were identified as hot spots for particulate matter and pollution indicators such as carbon monoxide.

The PSCF map for secondary aerosol source evaluated for Istanbul is shown in Fig. 9b. Ukraine, Poland, Belarus, Moldova, Slovakia, Hungary, Croatia, Bosnia, Albania, Romania, Bulgaria, and South Italy are identified as among the most important contributing countries for the secondary aerosol source above Istanbul. These potential source regions of secondary aerosol are in agreement with previous findings of Sciare et al. (2003) who reported that measured SO₂ and nss-SO₄²⁻ at a remote location in the eastern Mediterranean (Finokalia, Crete) predominantly originated from Central Europe, Hungary, Romania and Bulgaria. Besides, model study of Schaap et al. (2004) demonstrated the occurrence of the highest concentrations of secondary inorganic aerosol over the area between 47°N and 54°N. In the case of sulfate higher concentrations were observed over the Balkans, Germany, Poland and southeastern Europe, in agreement with emissions from EMEP for 2007. It is worth mentioning that local sources such as traffic (Markakis et al., 2009) are likely to contribute on observed pollutants in PM₁₀. In Turkey, about 33% of the power generation is obtained by fossil fuel (Bagdadioglu and Necmi Odyakmaz, 2009). Hence, particulate matter from these power plants might be suggested as another contributor from region itself.

3.4.2. PI of Istanbul on surrounding regions

Potential Impact map for pollution-1 is presented in Fig. 9c. As can be deduced from Fig. 9c the most likely areas to be affected by

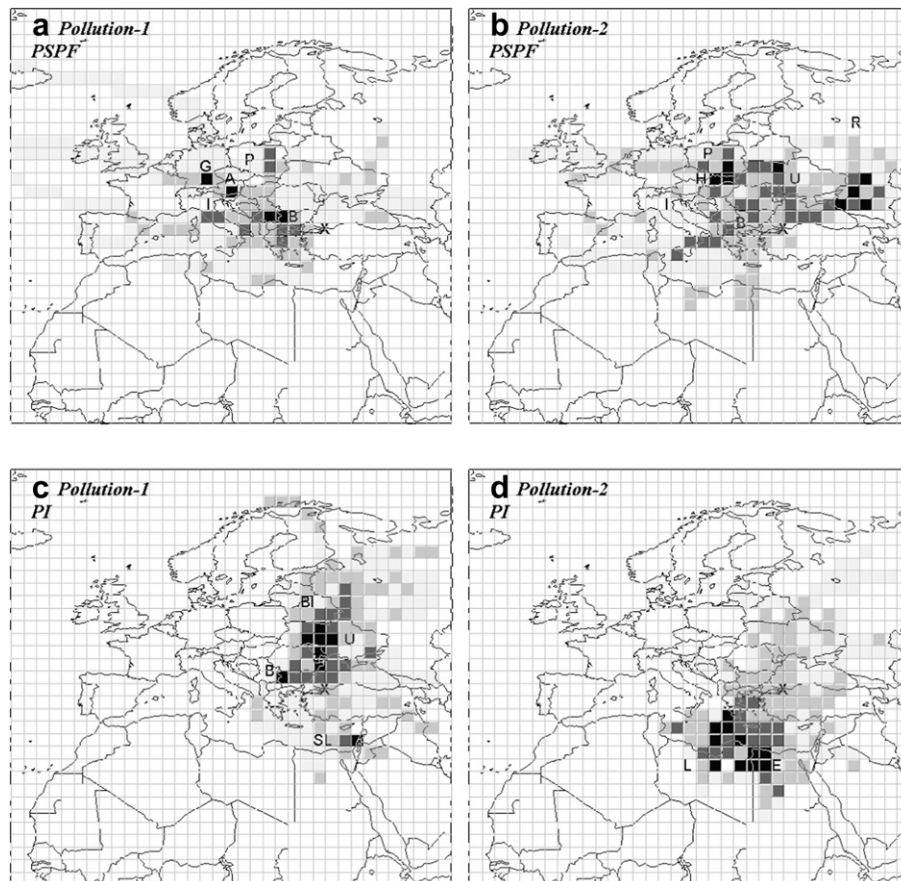


Fig. 9. Distribution of PSCF and PI (potential impact) values for pollution. (a) PSCF for Pollution-1 in winter, (b) PSCF for Pollution-2 in summer, (c) PI for Pollution-1 in summer and (d) PI for Pollution-2 in summer. X: Sampling site (Istanbul), A: Austria, B: Balkans, BI: Belarus, E: Egypt, G: Germany, I: Italy, L: Libya, U: Ukraine, R: Russia and SL: Southern Levantine Basin.

emissions from Istanbul in winter are located between 42° and 58° N and 22° E– 36° E. This area covers patches of the western Black Sea, Bulgaria, Romania, Moldova, Ukraine and Belarus. In addition, a small area over Southeastern Levantine Basin could be also affected by emissions from Istanbul. Whilst, PI map for pollution-2 (Fig. 9d) suggests that an area between 20° and 32° N and 18° E– 30° E (Fig. 9d) covering the Aegean and Levantine Sea, Greece, coastal sites of Libya and southeastern Egypt is under the potential influence of secondary particles originating from Istanbul. Various studies have shown that the atmosphere over the Aegean Sea in summer is mainly affected by the northern part of the Black Sea and Istanbul (Zerefos et al., 2000; Rappengluck et al., 2003; Sciare et al., 2003). Furthermore, above findings agree with results obtained by Lawrence et al. (2007). These authors studied regional pollution potentials of megacities and other major population centers using the 3-D global model MATCH (Model of Atmospheric Transport and Chemistry). Their results demonstrated that Istanbul has an outflow into the north during winter and an outflow mainly towards the south during summer.

4. Conclusions

Seven factors (secondary, refuse incineration, traffic, fuel oil, solid fuel, crustal and sea salt) are extracted applying PMF2 on PM_{10} samples collected in the megacity of Istanbul. The identified sources explain 98% of the total PM_{10} mass. In general, refuse incineration, solid fuel and traffic sources make larger contributions in winter than in summer and the transitional periods, accounting,

respectively, for 17.8, 18.8 and 28.5% of PM_{10} in winter. The crustal source shows statistically significant decreasing trend in the order of Transitional > Winter > Summer, with the highest contribution in transitional period (17%). Secondary aerosol source mean concentration is found to maximize in summer. Its contribution to PM_{10} is 1.6 and 5.3 times higher in summer (38.1%) than in transition (24.3%) and in winter (7.2%) periods.

During the sampling period, 42 events exceeded the limit value of $50 \mu\text{g m}^{-3}$. Source apportionment analyses denotes that PM_{10} exceedances are mainly due to anthropogenic sources (91%) and only 1% to natural ones. The remaining 8% has mixed origin.

Potential Source Contribution Function analysis highlights that trans-boundary aerosol transport actively takes place over a large area covering Europe, Eurasia and North Africa. Istanbul is affected mainly by Balkans and Western Europe then it delivers atmospheric particles over a large area including the western Black Sea, Bulgaria, Romania, Moldova, Ukraine and Belarus in winter. In summer, it receives secondary aerosol primarily from Eastern European countries which delivers into the atmosphere over the Aegean and Levantine Sea. Thus Istanbul emissions and regional meteorology may play an important role circulating the particles originating from itself and distant sources in this region.

Acknowledgments

The research leading to these results has received funding from the European Community's Seventh Framework Programme (FP7/2007-2013) under grant agreement no. 212095 (CityZen).

References

- Alpert, P., Ziv, B., 1989. The Sharav cyclone: observations and some theoretical considerations. *Journal of Geophysical Research* 94, 18495–18514.
- Andreae, T.W., Andreae, M.O., Ichoku, C., Maenhaut, W., Cafmayer, J., Karnieli, A., Orlovsky, L., 2002. Lightscattering by dust and anthropogenic aerosol at a remote site in the Negev desert, Israel. *Journal of Geophysical Research* 107 (D2). doi:10.1029/2001JD00252.
- Artinano, B., Querol, X., Salvador, P., Rodriguez, S., Alonso, D.G., Alastuey, A., 2001. Assessment of airborne particulate levels in Spain in relation to the new EU-directive. *Atmospheric Environment* 35, 43–53.
- Ashbaugh, L., Malm, W., Sadeh, W., 1985. A residence time probability analysis of sulfur concentrations at Grand Canyon national park. *Atmospheric Environment* 19, 1263–1270.
- Bagdadioglu, N., Necmi Odyakmaz, N., 2009. Turkish electricity reform. *Utilities Policy* 17, 144–152.
- Bardouki, H., Liakakou, H., Economou, C., Sciare, J., Smolik, J., Zdimal, V., Eleftheriadis, K., Lazaridis, M., Dye, C., Mihalopoulos, N., 2003. Chemical composition of size resolved atmospheric aerosols in the eastern Mediterranean during summer and winter. *Atmospheric Environment* 37, 195–208.
- Begum, B.A., Kim, E., Biswas, K.S., Hopke, P.K., 2004. Investigation of sources of atmospheric aerosol at urban and semi-urban areas in Bangladesh. *Atmospheric Environment* 38, 3025–3038.
- Birch, M.E., Cary, R.A., 1996. Elemental carbon-based method for monitoring occupational exposures to particulate diesel exhaust. *Aerosol Science and Technology* 25, 221–241.
- Brody, L.R., Nestor, M.J.R., 1980. Handbook for Forecasters in the Mediterranean, Part 2. Regional Forecasting Aids for the Mediterranean Basin. Naval Environmental Prediction Research Facility, Monterey, California (Technical Report TR 80-10), pp. VII-1–VII-13.
- Draxler, R.R., Hess, G.D., 1998. An overview of the HYSPLIT 4 modeling system for trajectories, dispersion and deposition. *Australian Meteorological Magazine* 47, 295–308.
- Duh, J.D., Shandas, V., Chang, H., George, L.A., 2008. Rates of urbanisation and the resiliency of air and water quality. *The Science of the Total Environment* 400, 238–256.
- Engelstaedter, S., Washington, R., 2007. Atmospheric controls on the annual cycle of north African dust. *Journal of Geophysical Research* 112 (D03103). doi:10.1029/2006JD007195.
- Favez, O., Cachier, H., Sciare, J., Alfaro, S.C., El-Araby, T.M., Harhash, M.A., Abdelwaha, M.M., 2008. Seasonality of major aerosol species and their transformations in Cairo megacity. *Atmospheric Environment* 42, 1503–1516.
- Gerasopoulos, E., Kouvarakis, G., Babasakalis, P., Vrekoussis, M., Putaud, J.P., Mihalopoulos, N., 2006. Origin and variability of particulate matter (PM₁₀) mass concentrations over the eastern Mediterranean. *Atmospheric Environment* 40, 4679–4690.
- Hien, P.D., Bac, V.T., Tinh, N.T.H., 2005. Investigation of sulfate and nitrate formation on mineral dust particles by receptor modeling. *Atmospheric Environment* 39, 7231–7239. <http://www.ceip.at/emission-data-webdb/emissions-used-in-emep-models/>.
- Huang, S., Rahn, K.A., Arimoto, R., 1999. Testing and optimizing two factor-analysis techniques on aerosol at Narragansett, Rhode Island. *Atmospheric Environment* 33, 2169–2185.
- Im, U., Markakis, K., Unal, A., Kindap, T., Poupkou, A., Incecik, S., Yenigun, O., Melas, D., Theodosi, C., Mihalopoulos, N., 2010. Study of a winter PM episode in Istanbul using the high resolution WRF/CMAQ modeling system. *Atmospheric Environment* 44, 3085–3094.
- Im, U., Tayanç, M., Yenigün, O., 2006. Analysis of major photochemical pollutants with meteorological factors for high ozone days in Istanbul, Turkey. *Water, Air, and Soil Pollution* 175, 335–359.
- Im, U., Tayanç, M., Yenigün, O., 2008. Interaction patterns of major photochemical pollutants in Istanbul, Turkey. *Atmospheric Research* 89, 382–390.
- Incecik, S., 1996. Investigation of atmospheric conditions in Istanbul leading to air pollution episodes. *Atmospheric Environment* 30, 2739–2749.
- Karaca, F., Camci, F., 2010. Distant source contributions to PM₁₀ profile evaluated by SOM based cluster analysis of air mass trajectory sets. *Atmospheric Environment* 44, 892–899.
- Karaca, M., Deniz, A., Tayanç, M., 2000. Cyclone track variability over Turkey in association with regional climate. *International Journal of Climatology* 20, 1225–1236.
- Karaca, F., Anil, I., Alagha, O., 2009. Long-range potential source contributions of episodic aerosol events to PM₁₀ profile of a megacity. *Atmospheric Environment* 43, 5713–5722.
- Kim, E., Hopke, P.K., 2006. Characterization of fine particle sources in the great smoky Mountains area. *The Science of the Total Environment* 368, 781–794.
- Kindap, T., Unal, A., Chen, S.H., Hu, Y., Odman, M.T., Karaca, M., 2006. Long-range aerosol transport from Europe to Istanbul, Turkey. *Atmospheric Environment* 40, 3536–3547.
- Koçak, M., Nimmo, M., Kubilay, N., Herut, B., 2004a. Spatio-temporal aerosol trace metal concentrations and sources in the Levantine basin of the eastern Mediterranean. *Atmospheric Environment* 38, 2133–2144.
- Koçak, M., Kubilay, N., Mihalopoulos, N., 2004b. Ionic composition of lower tropospheric aerosols at a north eastern Mediterranean site: implications regarding sources and long-range transport. *Atmospheric Environment* 38, 2067–2077.
- Koçak, M., Mihalopoulos, N., Kubilay, N., 2007a. Contributions of natural sources to high PM₁₀ and PM_{2.5} events in the eastern Mediterranean. *Atmospheric Environment* 41, 3806–3818.
- Koçak, M., Mihalopoulos, N., Kubilay, N., 2007b. Chemical composition of the fine and coarse fraction of aerosols in the north eastern Mediterranean. *Atmospheric Environment* 41, 7351–7368.
- Koçak, M., Mihalopoulos, N., Kubilay, N., 2009. Origin and source regions of PM₁₀ in the eastern Mediterranean atmosphere. *Atmospheric Research* 92, 464–474.
- Koulouri, E., Saarikoski, S., Theodosi, C., Markaki, Z., Gerasopoulos, E., Kouvarakis, G., Mäkelä, T., Hillamo, R., Mihalopoulos, N., 2008. Chemical composition and sources of fine and coarse aerosol particles in the eastern Mediterranean. *Atmospheric Environment* 42, 6542–6550.
- Kubilay, N., Saydam, C., 1995. Trace elements in atmospheric particulates over the eastern Mediterranean: concentration, sources and temporal variability. *Atmospheric Environment* 29, 2289–2300.
- Kubilay, N., Nickovic, S., Moulin, C., Dulac, F., 2000. An illustration of the transport and deposition of mineral dust onto the eastern Mediterranean. *Atmospheric Environment* 34, 1293–1303.
- Kubilay, N., Oğuz, T., Koçak, M., Torres, O., 2005. Ground-based assessment of total ozone mapping Spectrometer (TOMS) data for dust transport over the north eastern Mediterranean. *Global Biogeochemical Cycles* 19, GB1022. doi:10.1029/2004GB002370.
- Lawrence, M.G., Butler, T.M., Steinkamp, J., Gurjar, B.R., Lelieveld, J., 2007. Regional pollution potentials of megacities and other major population centers. *Atmospheric Chemistry and Physics* 7, 3969–3987.
- Lee, E., Chan, C.K., Pentti Paatero, P., 1999. Application of positive matrix factorization in source apportionment of particulate pollutants in Hong Kong. *Atmospheric Environment* 33, 3201–3212.
- Lim, J.M., Lee, J.H., Moon, J.H., Chung, Y.S., Kim, K.H., 2010. Source apportionment of PM₁₀ at a small industrial area using positive matrix factorization. *Atmospheric Research* 95, 88–100.
- Markakis K., Im U., Unal A., Dimitros M., Yenigun O., Incecik S., 2009. A computational approach for the compilation of high spatially and temporally resolved emission inventory for the greater Istanbul area. 7th International Conference on Air Quality - Science and Application (Air Quality 2009), Istanbul, 24–27 March 2009.
- Mihalopoulos, N., Kerminen, V.M., Kanakidou, K., Berresheim, H., Sciare, J., 2007. Formation of particulate sulfur species (sulfate and methanesulfonate) during summer over the eastern Mediterranean: a modelling approach. *Atmospheric Environment* 41, 6860–6871.
- Morishita, M., Keeler, G.J., Wagner, J.G., Harkema, J.R., 2006. Source identification of ambient PM_{2.5} during summer inhalation exposure studies in Detroit, MI. *Atmospheric Environment* 40, 3823–3834.
- Moulin, C., Lambert, E., Dayan, U., Masson, V., Ramonet, M., Bousquet, P., Legrand, M., Balkanski, Y.J., Guelle, W., Marticorena, B., Bergametti, G., Dulac, F., 1998. Satellite climatology of African dust transport in the Mediterranean atmosphere. *Journal of Geophysical Research* 103, 13137–13144.
- Paatero, P., 2007. User's Guide for Positive Matrix Factorization Programs PMF2 and PMF3, Part 1–2: tutorial. University of Helsinki, Helsinki, Finland.
- Paatero, P., Tapper, U., 1994. Positive matrix factorization: a non-negative factor model with optimal utilization of error estimates of data value. *Environmetrics* 5, 111–126.
- Polissar, A.V., Hopke, P.K., Paatero, P., Malm, W.C., Sisler, J.F., 1998. Atmospheric aerosol over Alaska 2. Elemental composition and sources. *Journal of Geophysical Research* 103 (D15), 19045–19057.
- Polissar, A.V., Hopke, P.K., Harris, J.M., 2001. Source regions for atmospheric aerosol measured at Barrow, Alaska. *Environmental Science and Technology* 35, 4214–4226.
- Raman, R.S., Hopke, P.K., 2007. Source apportionment of fine particles utilizing partially speciated carbonaceous aerosol data at two rural locations in New York State. *Atmospheric Environment* 41, 7923–7939.
- Rappengluck, B., Melas, D., Fabian, P., 2003. Evidence of the impact of urban plumes on remote sites in the eastern Mediterranean. *Atmospheric Environment* 37, 1853–1864.
- Rodriguez, S., Querol, X., Alastuey, A., Plana, F., 2002. Sources and processes affecting levels and composition of atmospheric aerosol in the western Mediterranean. *Journal of Geophysical Research* 107 (D24), 4777. doi:10.1029/2001JD001488.
- Schaap, M., Loon, M.V., Brink, H.M.T., Dentener, F.J., Builtjes, P.J.H., 2004. Secondary inorganic aerosol simulations for Europe with special attention to nitrate. *Atmospheric Chemistry and Physics* 4, 857–874.
- Sciare, J., Bardouki, H., Moulin, C., Mihalopoulos, N., 2003. Aerosol sources and their contribution to the chemical composition of aerosols in the eastern Mediterranean sea during summertime. *Atmospheric Chemistry and Physics* 3, 291–302.
- Tayanç, M., Im, U., Dogruel, M., Karaca, M., 2009. Climate change in Turkey for the last half century. *Climatic Change* 94, 483–502.
- Theodosi, C., Markaki, Z., Tselepidis, A., Mihalopoulos, N., 2010a. The significance of atmospheric inputs of soluble and particulate trace metals to the eastern Mediterranean seawater. *Marine Chemistry* 120, 100–107.
- Theodosi, C., Im, U., Bougiatioti, A., Zarrmpas, P., Yenigun, O., Mihalopoulos, N., 2010b. Aerosol chemical composition over Istanbul. *The Science of the Total Environment* 408, 2482–2491.
- TUIK (Turkish Statistical Institution), 2007. Addressed based population registration system population census.

- Viana, M., Pandolfi, M., Minguillon, M.C., Querol, X., Alastuey, A., Monfort, E., Celades, I., 2008. Inter-comparison of receptor models for PM sources apportionment: case study in an industrial area. *Atmospheric Environment* 42, 3820–3832.
- Visschedijk, A.J.H., Zandveld, P.Y.J., Denier van der Gon, H., 2007. High resolution gridded European emission database for the EU integrate project GEMS TNO-report 2007-A-R0233/B.
- Wedepohl, K.H., 1995. The composition of the continental crust. *Geochemica Cosmochimica Acta* 59, 1217–1232.
- Yusuf, A.A., Resosudarmo, B.P., 2009. Does clean air matter in developing countries' megacities? A hedonic price analysis of the Jakarta housing market, Indonesia. *Ecological Economics* 68, 1398–1407.
- Zerefos, C., Ganev, K., Kourtidis, K., Tzortsiou, M., Vasaras, A., Syrakov, E., 2000. On the origin of SO₂ above northern Greece. *Geophysical Research Letters* 27, 365–368.